Solar Cycle Dependency of Sun-as-a-Star Photospheric Spectral Line Profiles

Luca Bertello[1], Alexei A. Pevtsov[2], Mark S. Giampapa[1], Andrew R. Marble[1]

[1]*National Solar Observatory, 950 North Cherry Ave., Tucson, Arizona, USA 85719*

[2]*National Solar Observatory, Sunspot, New Mexico, USA 88349*

Abstract. We investigate solar-cycle related changes in the profile of several photospheric spectral lines taken with the Integrated Sunlight Spectrometer (ISS) operating at the National Solar Observatory at Kitt Peak (Arizona). ISS, which is one of three instruments comprising the Synoptic Optical Long-term Investigations of the Sun (SOLIS) facility, is designed to obtain high spectral resolution (R = 300,000) observations of the Sun-as-a-star in a broad range of wavelengths (350 nm - 1100 nm). Daily measurements were obtained since December 2006, covering the decline of solar cycle 23 and the rising phase of cycle 24. We present time series of line parameters and discuss their correlation to indices of solar magnetic activity. Because of their different response to variations in the thermodynamic and magnetic structures of the solar atmosphere, the measured line shape parameters provide an excellent tool for disentangling thermal and magnetic effects occurring during different phases of the solar cycle. The results of this analysis may also help with developing a better understanding of magnetic cycles of activity in other solar-like stars.

1. Introduction

The diagnostic value of the Fraunhofer spectral lines to probe the conditions of the solar atmosphere was established a long time ago. Changes in the observed profile of these lines provide significant information about the velocity fields and properties of the magnetized plasma in the atmospheres of the Sun and other stars. For example, convective motions in the photospheres of the Sun/stars produce asymmetries in spectral lines because brightness differences are coupled to the flow velocities (e.g., Voigt 1956; Ridgway & Friel 1981). A

standard metric for measuring the asymmetry of spectral lines is given by its bisector. The bisector is defined as the line half-way between points of equal intensity on the line profile. The details of bisector shapes vary across the H-R diagram (e.g., Gray 2005b). A curvature reminiscent of a distorted letter C is common for stars on the cool half of the H-R diagram, while bisectors for hotter stars have a reversed-C shape (Gray & Toner 1986; Gray 2005a).

Variations in the shape of magnetically sensitive lines can be used to detect changes in the thermodynamic properties of the plasma and global magnetic field (e.g. Fabbian et al. 2010; Livingston et al. 2007; Penza et al. 2004; Criscuoli et al. 2013). However, these changes are particularly difficult to detect in Sun-as-a-star and stellar observations due to the very small magnitude of these effects.

The Integrated Sunlight Spectrometer (ISS) operating at the National Solar Observatory at Kitt Peak (Arizona) is designed to obtain high spectral resolution (R $\cong$ 300,000) observations of the Sun-as-a-star in a broad range of wavelengths (350 nm -1100 nm). Beginning December 1, 2006, the ISS has been taking daily observations in nine spectral bands centered at the CN bandhead at 388.40 nm, Ca II H at 396.85 nm, Ca II K at 393.37 nm, C I at 538.00, Mn I at 539.41 nm, H-α at 656.30 nm, Ca II at 854.19 nm, He I at 1083.02 nm, and NaD1 at 589.59 nm. Beginning January 7, 2008, C I 538.00 nm spectra superimposed with reference lines from an iodine vapor cell have been additionally included. Table .1 lists currently observed spectral lines.

Table .1: Spectral bands measured by the ISS instrument

Spectral band	λ_0, nm	$\Delta\lambda$, nm	$d\lambda/dx$, pm/pixel	Start date
CN	388.40	0.58	0.564	December 4, 2006
Ca II K	393.37	0.55	0.541	December 1, 2006
Ca II H	396.85	0.53	0.522	December 4, 2006
C I	538.00	0.84	0.824	December 4, 2006
C I (with iodine lines)	538.00	0.84	0.824	January 7, 2008
Mn I	539.41	0.83	0.816	December 4, 2006
NaD1	589.59	0.98	0.956	March 23, 2011
H-alpha	656.30	1.14	1.12	August 31, 2007
Ca II	854.19	1.61	1.58	December 13, 2006
He I	1083.02	1.65	1.61	December 4, 2006

Notes to Table 1.*: Each spectral band is centered at λ_0, with a bandwidth given by $\Delta\lambda$. The average linear dispersion over time, $d\lambda/dx$, is also given. The start date (fifth column) indicates the first day ISS began to observe in that particular spectral band.*

Additional information about ISS, including transmission characteristics of the fiber optics, the instrument's block diagram, and its mechanical and optical layout are available

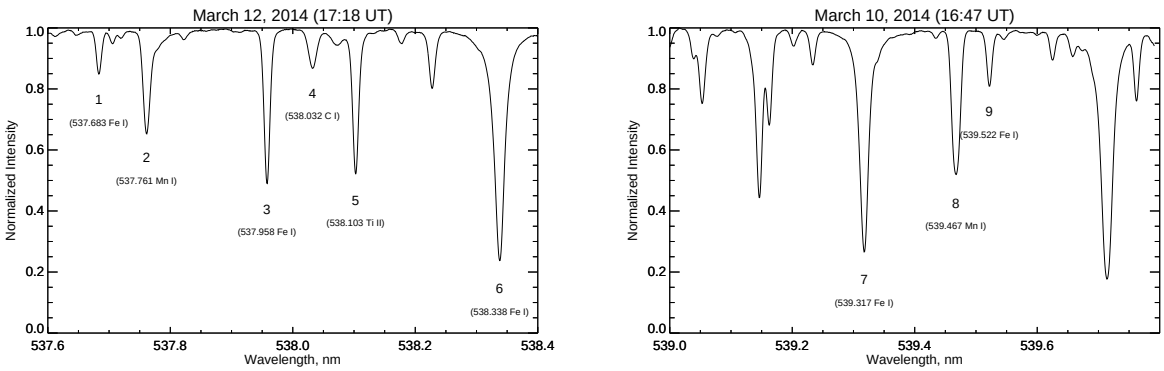

Figure .1: ISS C I (left) and Mn I (right) bands. The spectral sampling is about 8.2 mÅ. The numbers refer to the spectral lines used in this study and their properties are listed in Table .2.

from the SOLIS web site at http://solis.nso.edu/ISSOverview.html. Daily observations can be accessed from http://solis.nso.edu/0/iss.

Criscuoli et al. (2013) have investigated the effect of magnetic features on the shape of two Fe I magnetically sensitive lines (630.2 nm and 617.3 nm) using high-resolution spectropolarimetric data acquired with the Interferometric Bidimensional Spectrometer (IBIS; Cavallini 2006) at the Dunn Solar Telescope (NSO at Sacramento Peak). Their results show that the central intensity of these lines is sensitive to both temperature and magnetic flux density variations, the full width at half maximum (FWHM) is mostly affected by magnetic field changes, and the equivalent width (EQW) is mostly sensitive to temperature. This implies that it is possible to disentangle magnetic from purely thermodynamic effects by comparing time series of these parameters. The objective of our investigation is to extend this idea to disk-integrated solar measurements and possibly determine a correlation between temporal variations in the solar global magnetic field and corresponding variations in line shape parameters. The outcome of this study may offer important clues about possible new approaches to determining the magnetic field properties in other stars. We present here some very preliminary results from this investigation.

2. Data Analysis

For this study, we investigated the temporal behavior of a set of photospheric lines extracted from the ISS bands centered at C I 538.00 nm and Mn I 539.41 nm spectral lines. Figure .1 shows typical ISS observations taken in these two bands, where the lines investigated here are marked by a number. The set includes spectral lines of different strength and magnetic sensitivity, as listed in Table .2.

The wavelength- and flux-calibration of both the ISS C I and Mn I data were performed following the approach described in Pevtsov et al. (2014), using the NSO Fourier Transform Spectrometer (FTS; Wallace, Hinkle & Livingston 2007) spectral atlas as a reference. In brief, a second order (i.e., linear dispersion) wavelength solution was obtained by cross-correlating the regions of the ISS and FTS spectra with absorption features. Simultaneously,

Table .2: List of spectral lines

no.	λ_0 (nm)	Elem.	Transition	Low EP (eV)	High EP (eV)	$g_{\rm eff}$	$I_{\rm core}$	EQW (mÅ)
1	537.6833	Fe I	b^1D2_2 - $v^3P^\circ_1$	4.29	6.60	0.750	0.85	13
2	537.7612	Mn I	$z^4P^\circ_{5/2}$- $e^4S_{3/2}$	3.83	6.12	1.300	0.65	45
3	537.9579	Fe I	b^1G2_4 - $z^1H^\circ_5$	3.69	6.00	1.000	0.49	56
4	538.0323	C I	$^1P^\circ_1$ - $^1P_1$	7.68	9.99	1.000	0.87	26
5	538.1026	Ti II	$b^2D2_{3/2}$ - $z^2F^\circ_{5/2}$	1.57	3.87	0.900	0.52	56
6	538.3379	Fe I	$z^5G^\circ_5$ - e^5H_6	4.31	6.61	1.083	0.23	204
7	539.3174	Fe I	$z^5D^\circ_3$ - e^5D_4	3.24	5.54	1.500	0.26	153
8	539.4672	Mn I	$a^6S_{5/2}$ - $z^8P^\circ_{7/2}$	0.00	2.30	1.857	0.51	74
9	539.5218	Fe I	$z^5G^\circ_2$ - g^5F_1	4.45	6.74	0.500	0.81	20

Notes to Table 2.*:* λ_0 *is the reference wavelength, the central intensity* $I_{\rm core}$ *is the median value determined from all the ISS measurements, and EQW is the equivalent width. The effective Landé factor* $g_{\rm eff}$ *was computed using the formula given in Landi Degl'Innocenti (1982), while the other quantities are from the National Institute of Standards and Technology (NIST) website (http://www.nist.gov/pml/data/asd.cfm).*

a third order flux-calibration curve was fit via least-squares minimization of the spectra within continuum windows between those features.

For each line listed in the table we extracted from the observed profile a set of parameters and studied their behavior with respect to the solar cycle of activity. The parameters are: FWHM, EQW, core intensity ($I_{\rm core}$), and line asymmetry. The bisector of a spectral line is routinely used to characterize its asymmetry. For this study, we used the wavelength position of the bisector at three different relative intensity levels (25%, 50%, and 75% from the core intensity). The core intensity is determined from a 9-point quadratic fit of the bottom of the profile, while the FWHM and bisector were computed via cubic spline interpolation at the proper intensity levels. The EQW is determined by numerically integrating

$$\mathrm{EQW} = \int (1 - I_\lambda) d\lambda$$

over a selected wavelength range of interest centered on the line core, and with the assumption that the continuum intensity is equal to one. Since we are interested in relative variations of EQW, the actual extension of this range is not critical. Finally, it is important to point out that, because of the adopted calibration, the central wavelength positions of these lines is constrained to be the same as those of the FTS spectrum used as a reference. That is, these central wavelength positions will not change with time.

3. Results

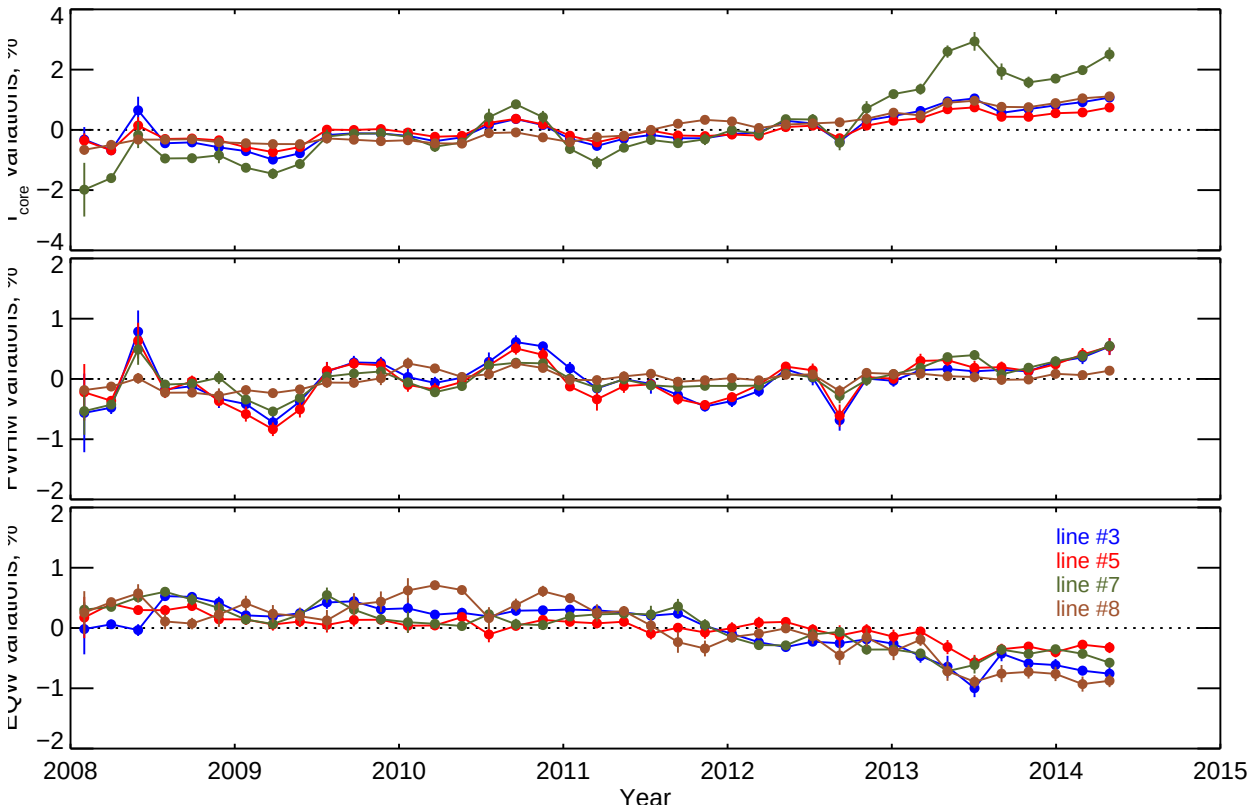

Figure .2: Variations in core residual intensity (I_{core}), FWHM, and equivalent width (EQW) for four of the nine spectral lines investigated in this study. Data were averaged in 60-day intervals, and the variations are computed with respect to the median value of the original time series. The error bars are 3-σ of the mean.

Figure .2 shows the variations with the cycle of solar activity of three of the four line parameters investigated. For clarity, we plot here only the results for some of the strongest lines in the set. These lines exhibit a systematic increase in I_{core} of about 4-5% (e.g., line #7) and a systematic decrease in EQW of about 1% during the rising phase of cycle 24. On the other hand, the FWHM does not present any significant long-term trends with the cycle of activity. Shallow lines (e.g., #1, #4, and #9), not shown here, exhibit very little or insignificant variations in these parameters. One interesting feature shown in Figure .2 is the presence of an annual modulation in the I_{core} and FWHM time series, quite visible during the period ∼2008 - 2011.

This modulation seems to be in phase with the annual variation of the B_0 angle - the heliographic latitude of the centre of the solar disk - as shown in Figure .3, suggesting that it may be caused by the Earth's orbital motion around the Sun. This effect is more prominent during periods of minimal solar activity when the poloidal field is the major magnetic contributor affecting the line shape and at times of extreme B_0 angle values (when

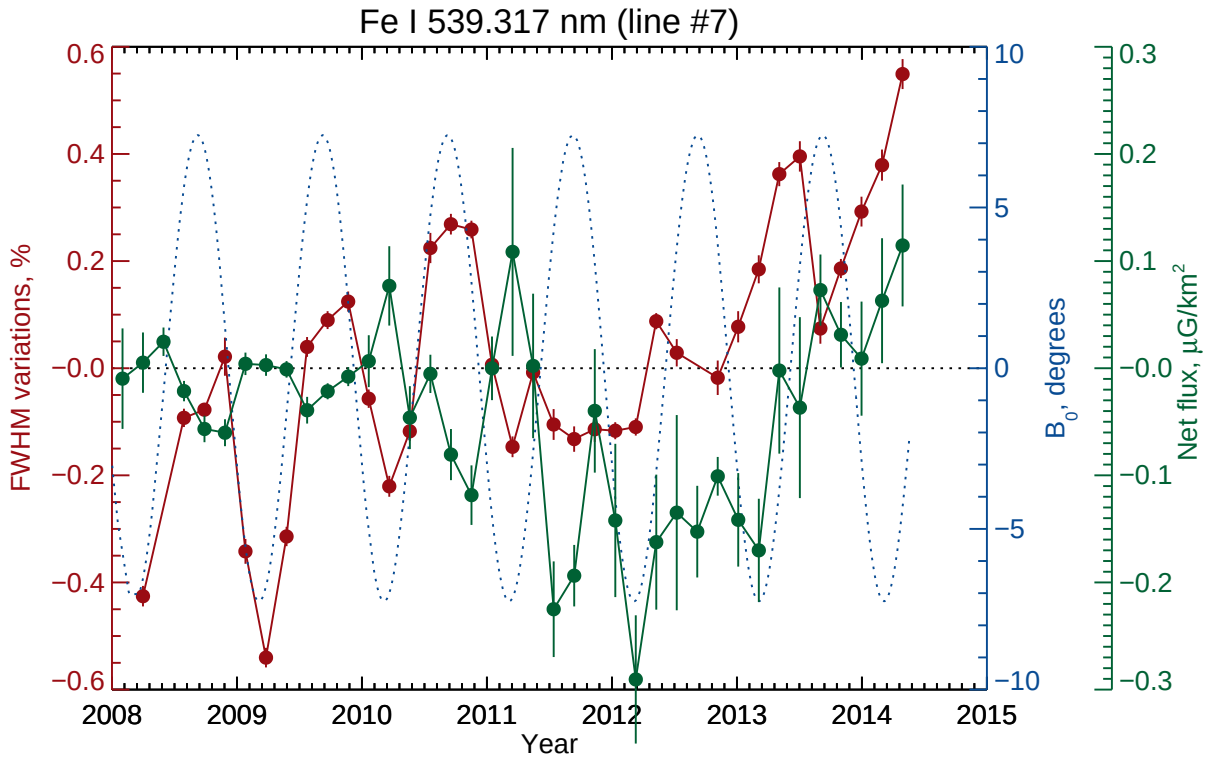

Figure .3: Comparison between variations in the FWHM of one of the strongest lines used in this investigation (red points) and the net magnetic flux computed at 630.15 nm from SOLIS Vector Spectromagnetograph observations (green points). Data were averaged in 60-day intervals, and the error bars for both sets of points are the standard deviation of the mean. Also shown in blue, as a reference, are the variations of the heliographic latitude of the central point of the solar disk (B_0).

one of the Sun's poles is observed). Once the overall level of magnetic activity rises and the toroidal field becomes predominant, the activity moves to lower latitudinal bands and the sensitivity to variations in the B_0 angle is strongly reduced. The fact that the annual variations disappear after 2011 indicates that these variations are of solar origin, and not caused by the Earth's orbital motion. The rise in solar activity can explain the quasi-systematic increase in FWHM after 2011. To further validate this idea, we also plot in Figure .3 the average values of the net magnetic flux computed from daily SOLIS VSM full-disk magnetograms taken in the Fe I 630.15 nm spectral line for the same period of time covered by the ISS observations. Although not quite as evident as for the case of the FWHM, the net magnetic flux exhibits a similar modulation around zero during the years 2008 to 2011. After 2011, the net flux is mostly negative until it reverses its sign around the middle of 2013. The good overall agreement between the behavior of the FWHM and the net magnetic flux is another indication that some of the line shape parameters investigated

here, as measured by the ISS instrument, are very sensitive to variations in the solar global magnetic field.

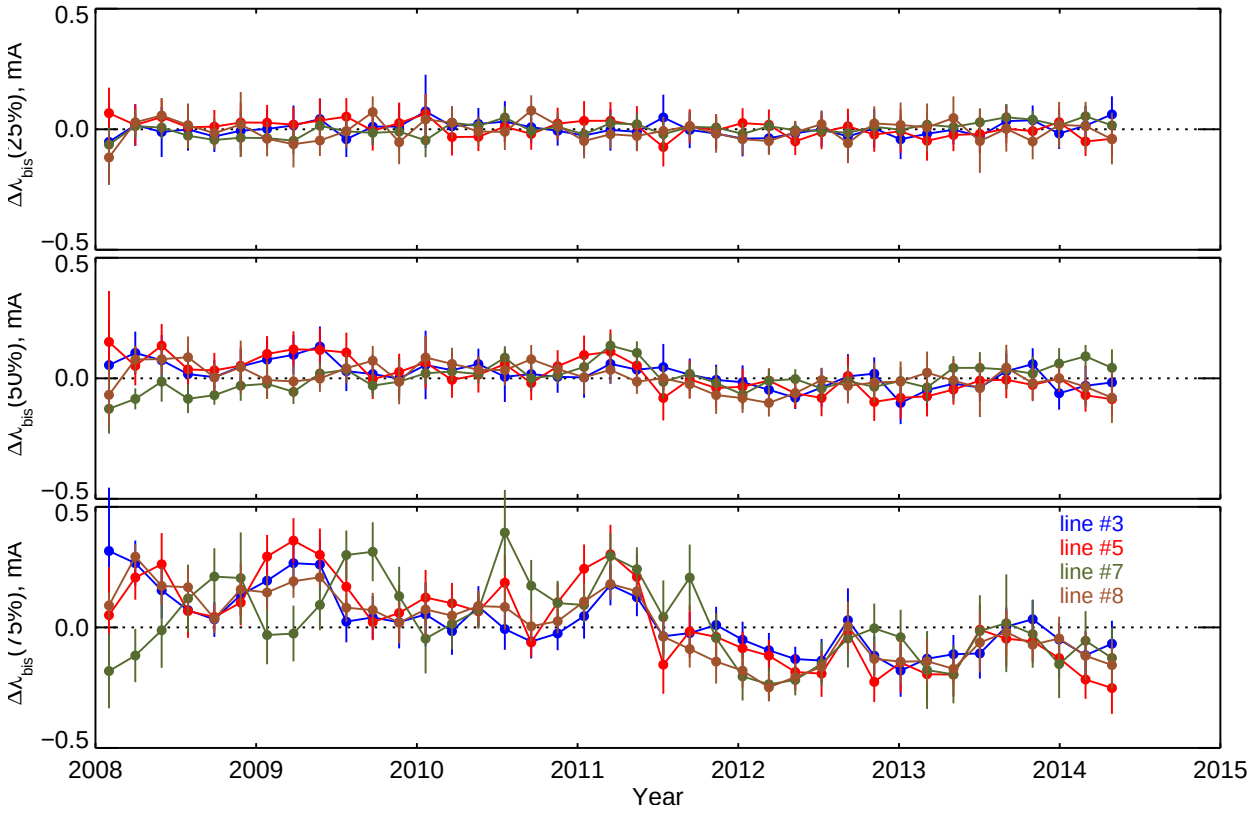

Figure .4: Variations in the line bisector for the same four lines discussed in Figure .2. The wavelength position of the line bisector is computed at three different relative intensity levels: $I_i = f_i(1 - I_{core}) + I_{core}$, with $f_i = \{0.25, 0.50, 0.75\}$. Corresponding variations are computed from the formula $\Delta\lambda_{bis}(I_i, t) = \lambda_{bis}(I_i, t) - \text{median}(\lambda_{bis}(I_i, t))$. Data are averaged in 60-day intervals.

Figures .4 shows the results from the analysis of the line bisector. All the lines investigated here preserve their asymmetry during the cycle of activity up to about a 50% level of their residual intensity. A slight change of asymmetry (fraction of mÅ) is detected at higher intensity levels. Some of these changes may be due to the contamination of nearby telluric lines that typically have seasonal variations. However, there is a clear systematic change in asymmetry close to the continuum occurring around the middle of 2011. The change in sign of $\Delta\lambda_{bis}(75\%)$, from positive to negative, indicates that the line profiles tend to become more symmetric with the overall increase in solar activity.

Of the pool of spectral lines examined in this study, the Mn I 539.467 nm line is one that has received considerable attention in the past (e.g. Livingston & Wallace 1987; Malanushenko et al. 2004; Livingston et al. 2007). This spectral line presents an unusual sensitivity to solar activity, due, most likely, to its excessive hyperfine structure (Vitas et al. 2009). For example, Livingston & Wallace (1987) have noted that the EQW of this

line correlates quite well with the chromospheric Ca II K core intensity during the period 1976 to 1985. Figure .5 show a very similar trend with the solar cycle between the intensity variations in the core of Mn I 539.467 nm and the Ca II K 1-Å emission index. While Fig. 5 would appear to suggest that the variations in Mn I are a direct result of chromospheric heating, Vitas et al. (2009) pointed out that variability in the Mn I 539.467 nm line is in fact dominated by magnetic concentrations that constitute on-disk network and plage combined with the its Zeeman sensitivity but is not affected by chromospheric heating. Therefore, the correlation in Fig. .5 is the result of the separate correlations of the Ca II K core and the Mn I core, respectively, with magnetic field strength and area coverage.

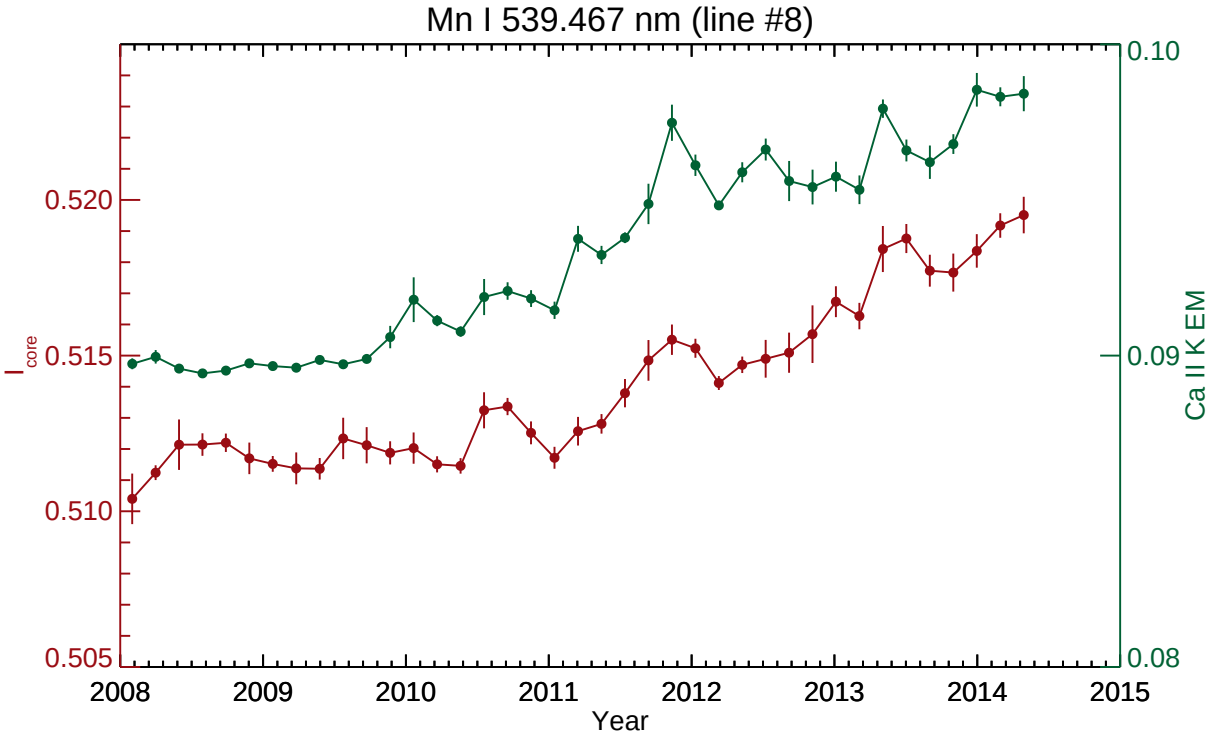

Figure .5: Intensity variations in the core of Mn I 539.467 nm and their correlation with the chromospheric ISS Ca II K 1-Å emission index (EM). Error bars in both sets are 3 standard deviations of the mean value. The good correlation between these two parameters indicates that the core of this line is a good proxy for monitoring chromospheric activity in the Sun and, maybe, in solar-like stars.

4. Conclusions

Shallow lines show very little or insignificant variations in the line core relative intensity with respect to the cycle of solar activity, while stronger lines exhibit a systematic increase of about

4-5% (e.g. line #7). The EQW shows a systematic decrease of about 1% for the strongest lines during the rising phase of cycle 24. This dependency of the line profile parameters on the magnetic field is consistent with the results published in Criscuoli et al. (2013). The analysis of the line bisectors indicates that all the lines maintain their asymmetry during the cycle of activity, at least up to the 50% level of their residual intensity. A slight change of asymmetry (fraction of mÅ) is detected at relative intensity levels closer to the continuum.

During the period ∼2008-2011, the variations in FWHM are quite well correlated with the variations in B_0 and anticorrelated with the net magnetic flux. This is mainly because of the contribution of the polar fields. After ∼2012, the FWHM increases with the rising level of solar activity. One line from our set, Mn I 539.467 nm, exhibits properties in its core intensity that are very similar to the behavior of the 1-Å emission index of the well studied Ca II K chromospheric line. Finally, from a visual inspection of the top panel of Figure .2, we note that the strong spectral line Fe I 539.3174 nm (line #7) shows the largest variations in its core intensity among all the lines investigated by this study.

Acknowledgements. The authors thank the organizers of the 18th "Cool Stars" Workshop for their hospitality. This work utilizes SOLIS data obtained by the NSO Integrated Synoptic Program (NISP), managed by the National Solar Observatory, which is operated by the Association of Universities for Research in Astronomy (AURA), Inc. under a cooperative agreement with the National Science Foundation.

References

Cavallini, F. 2006, Solar Phys., 236, 415

Criscuoli, S., Ermolli, I., Uitenbroek, H., & Giorgi, F. 2013, ApJ, 763, 144

Fabbian, D., Khomenko, E., Moreno-Insertis, F., & Nordlund, Å. 2010, ApJ, 724, 1536

Gray, D. F. 2005a, PASP, 117, 711

Gray, D. F. 2005b, "The Observation and Analysis of Stellar Photospheres, 3rd Edition, by D.F. Gray. ISBN 0521851866

Gray, D. F., & Toner, C. G. 1986, ApJ, 310, 277

Landi Degl'Innocenti, E. 1982, Solar Phys., 77, 285

Livingston, W., & Wallace, L. 1987, ApJ, 314, 808

Livingston, W., Wallace, L., White, O. R., & Giampapa, M. S. 2007, ApJ, 657, 1137

Malanushenko, O., Jones, H. P., & Livingston, W. 2004, in Multi-Wavelength Investigations of Solar Activity, ed. A. V. Stepanov, E. E. Benevolenskaya & A. G. Kosovichev, IAU Symp., 223, 645

Penza, V., Caccin, B., & Del Moro, D. 2004, A&A, 427, 345

Pevtsov, A. A., Bertello, L., & Marble, A. R. 2014, Astronomische Nachrichten, 335, 21

Ridgway, S. T., & Friel, E. D. 1981, IAU Colloq. 59: Effects of Mass Loss on Stellar Evolution, 89, 119

Vitas, N., Viticchiè, B., Rutten, R. J., Voumlgler, A. 2009, A&A, 499, 301

Voigt, H.-H. 1956, Zeitschrift für Astroph., 40, 157

Wallace, L., Hinkle, K., & Livingston, W. 2007, Advances in Solid State Physics

Cool Stars as Planet Hosts